Iraqi Journal of Physics, 2023

https://doi.org/10.30723/ijp.v21i3.1128

Vol. 21 No. 3, PP. 55-63
P-ISSN: 2070-4003
E-ISSN: 2664-5548

Enhancing the Spectral Characteristics of Rhodamine 610 Laser Dye Doped with Chemically Prepared Gold Nanoparticles

Abu-Al-Hassan H. Ali[1a*] and Falah A-H. Mutlak[1b]
[1]*Department of physics, college of Science, University of Baghdad, Baghdad, Iraq*
[b]E-mail: falah.mutlak@.sc.uobaghdad.edu.iq
[a*]Corresponding author: aboalhasan.hatem1204a@sc.uobaghdad.edu.iq

Abstract

In this study, gold nanoparticle samples were prepared by the chemical reduction method (seed-growth) with 4 ratios (10, 12, 15 and 18) ml of seed, and the growth was stationary at 40 ml. The optical and structural properties of these samples were studied. The 18 ml seed sample showed the highest absorbance. The X- ray diffraction (XRD) patterns of these samples showed clear peaks at (38.25^o, 44.5^o, 64.4^o, and 77.95^o). The UV-visible showed that the absorbance of all the samples was in the same range as the standard AuNPs. The field emission-scanning electron microscope (FE-SEM) showed the shape of AuNPs as nanorods and the particle size between 30-50 nm. Rhodamine-610 (RhB) was prepared at 10^{-5} M concentration, the optical measurements were studied, AuNPs and RhB were mixed at ratios (1:1, 1:2, 1:3), and the fluorescence measurements were done. Full width at half maximum (FHWM) and the intensity of RhB after mixing were changed, and this result showed significant efficacy for many applications. The study shows that this mixing could be used after doping with polymer as a random gain medium or saturation absorber for pulse laser generation.

Article Info.

Keywords:
dye laser, gold nanoparticle, rhodamine B, chemical synthesis, fluorescence.

Article history:
Received: Apr. 29,2023
Revised: Jun. 30, 2023
Accepted: Jul. 13, 2023
Published: Sep. 01,2023

1. Introduction

Nanoparticle-sized materials exhibit different size-related characteristics that distinguish them from their bulk equivalents, such as enormous surface areas [1, 2], unusual magnetic properties [3, 4], and interactions with light [4, 5]. Nanoparticles have three physical dimensions that are on the nanometer scale. Dimensions and morphology of gold nanoparticle impact show apparent color, light wavelengths transmitted/absorbed, and the possibility of light scattering [6, 7].

Plasmons, defined as collective oscillations of loosely bound electrons in response to electromagnetic waves, give gold nanoparticle suspensions their vibrant colors. When the frequency of the plasmon and the incident light wave coincide [8, 9], it may be recognized by the spectra's scattering and absorption peaks, which correspond to various wavelength ranges. By altering the quantity of the reactant during the synthesis process, which results in a broad spectrum range from the visible (600 nm) to the near-infrared area, the aspect ratio of gold nanorods (AuNRs) may be dramatically modified. Furthermore, theoretical calculations and practical findings show that the localized surface plasmon resonance (LSPR) directly affects the aspect ratio (length/diameter) of AuNRs, with the longitudinal LSPR contributing the most [10, 11]. When comparing the different approaches to the chemical synthesis of AuNPs, the Turkevich technique is promising. In the Turkevich method, a mild reducing agent, such as citrate, ascorbic acid, or tannic acid, reduces Au^{3+} ions in an aqueous solution. Gold nanoparticles (AuNPs) produced with this method are biocompatible and rather modest in size. The main drawback of this method is the stringent regulation process (temperature, concentration, and pH) that must be followed in order to produce monodisperse particles of the correct sizes. Furthermore, tagging AuNPs with organic drug molecules and surface modification with diverse ligands are difficult in a pure aqueous medium

due to the organic component's poor solubility and hydrophobicity in water [12-14]. Then, by enhancing the Turkevich strategy, resolution is prioritized [15].

Organic dye-based active laser media have a wide stimulated-emission cross-section, a high gain, and a broad fluorescence spectrum, which are all good things. They may be employed as sources to produce femtosecond and picosecond laser pulses using simple cavities [16-18]. One of the main issues with such dye gain media is the disintegration of the optical bleaching of dye molecule components. Such systems often employ a circulating dye setup to improve laser quality, which increases the complexity and undesirable environmental impact of the device. Doping polymers and other solid-state materials with laser dyes and modified silica glass, among others, increased in the 1990s [19]. But these media haven't received much attention lately due to their weak effectiveness and fast deterioration. However, the stability of the solid host and the interaction between the dye and the host are now key factors in the stability of the laser emission. In general, three factors contribute to the loss of laser medium quality: the synthesis of new molecules or clusters that result in non-radiative absorption; the oxidation of dye molecules at higher levels; and the harm light-to-heat conversion causes to dye molecules. To slow dye deterioration, holes in the laser host can be filled with low-mass molecules with high heat conductivity [19].

Gold nanoparticles have recently attracted interest due to their great heat conductivity and broad visible-spectrum absorption [20]. It is possible to enhance the thermal and photophysical characteristics of dye-doped solid-state gain media by creating a composite organic-inorganic matrix. Such samples created from suspensions with different dye and nanoparticle compositions were evaluated by the laser Cerdanb for their performance compositions. In metallic nanoparticles, a host solid-state dye, the laser's electromagnetic field can be altered by particles such as gold nanoparticles (AuNPs) [21].

In this research, AuNPs were created using a seed-growth methodology and their structure and characteristics were investigated. In contrast to most investigations that have employed silver as seeds, our study utilized gold. One advantage of utilizing gold (Au) seeds instead of silver (Ag) seeds is the ability to control the morphology of the resulting nanoparticles (NPs) by manipulating the quantity of Au seeds. Active laser media depending on organic dyes could be used to generate ultrashort laser pulses in the picosecond and femtosecond ranges utilizing straightforward cavities.

2. Experimental Work

2.1 Gold Preparation

The first step is called seed, which is obtained by using 50 ml of 0.015 mM chlorauric acid solution mixed with 20 ml of 0.1M sodium citrate. After that, 0.6 ml of ice-cold 0.01 M sodium borohydride solution was added to the mixture. Stirring the seed solution was continued for 2 min, the solution turned orange-red immediately after adding $NaBH_4$, which refers to AuNPs formation. This solution was kept at room temperature for 2hr. [22-26].

The second step is to prepare “the growth solution” obtained by mixing 200 ml of 0.05mM-chlorauric acid solution with 40 ml of 0.1M-CTAB. Initially, a solution containing 10 ml of 0.01 M $AgNO_3$, 10ml of 0.01 M $HAuCl_4$, and 100 ml of 0.1 M CTAB was produced. In a water bath, the CTAB solution was heated to 30^o C. In a test tube, 3 mL of 0.1 M CTAB was added, to which Milli-Q water (1.748 ml), $HAuCl_4$ (200 mL), and ascorbic acid (32 ml) were added one at a time. After each addition, the mixture was gently stirred. After waiting 4 seconds, 20 ml of 0.01 M silver nitrate was poured into the test tube and carefully mixed. The created solution was put in a water

bath at 30°C; it took three hours for the reaction to finish. The solution was then kept at room temperature after being centrifuged twice at 4500 rmp for 5 minutes each time [27]. Four concentrations were prepared by taking (10, 12, 15, and 18) ml from seed and a growth stationary of 40ml.

2.2 Dye Preparation

Rhodamine-610 (RhB) (from Lambda Physik) was produced in this work using the formulae for preparation and dilution. Several dye molar concentrations (10^{-2}, 10^{-3}, 10^{-4}, 10^{-5}, 10^{-6}) M were prepared by dissolving the dye solution in an ethanol solvent. While preparing, use dilution and preparation formulas, whether absorbance or fluorescence, to lower the error rate. To find the ideal concentration and solvent absorption, fluorescence spectra were taken. With RhB dye, we believed that a concentration of 10^{-5} M was the best since it produced the highest fluorescence intensity and the lowest full width at half maximum (FWHM). Spectrophotometry of the dye solutions was determined by a computer-controlled Shimadzu UV-Visible spectrophotometer 1800 in the spectral range 200-800 nm and fluorescence spectral using Shimadzu 6000 with 532 nm exaction flash lambs was obtained. After preparing the Au NPs and the dye separately, mix the Au NPs with the dye in a ratio (1:1, 1:2, and 1:3).

3. Results and Discussion

The crystallinity of the generated AuNPs was investigated using the X-ray diffraction (XRD) technique; the XRD patterns are displayed in Fig. 1. At 18-seed concentration, the gold nanocrystals XRD pattern showed four different peaks at 2θ = 38.25°, 45.5°, 64.4°, and 77.95°. All four peaks were consistent with the face center cubic [FCC] of the lattice's conventional Bragg reflections (111), (200), (220), and (311). The strong diffraction at peak 38.25° demonstrates that zero-valent gold's preferred growth orientation was locked in the (111) direction. This is used to describe solids when the molecules used to make them are three-dimensional patterns made of similarly spaced atoms or molecules. Pure Au nanocrystals often exhibit this XRD pattern. Gold has very similar lattice constants (JCPDS 4-0783). The properties of the generated AuNPs are listed in Table 1. On average, the lattice constant (a) was equal to 3.6. [28, 29].

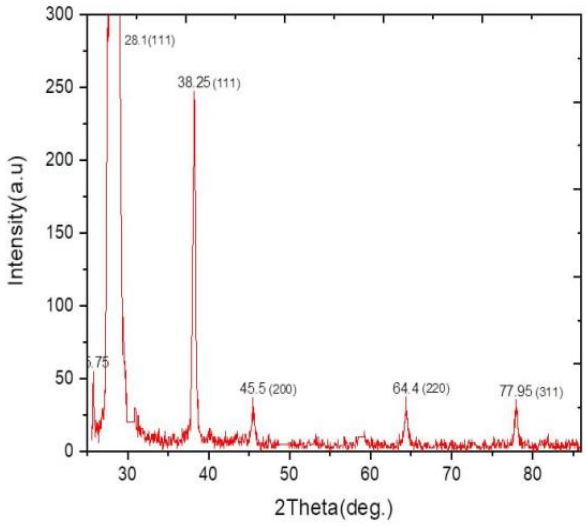

Figure 1: XRD pattern of Au nanoparticles at 18-seed concentration.

Table 1: Properties of Au NPs measuring form XRD pattern

Miller indices (hkl)	2θ (deg)	FWHM (rad)	D (nm)	d-spacing (A^o)	a (A^o)
111	38.25	0.006578146	22.283821	2.365096185	3.987
200	44.5	0.007864454	19.007667	2.055489715	4.110
200	64.4	0.008285078	19.726323	1.453051534	2.800
311	77.95	0.008459611	20.934783	1.236918708	3.979

It is clear from the Field Emission- Scanning Electron Microscope (FE-SEM) image at 10 μm magnification (Fig. 2) that the shape of the AuNPs is nanorod. At 500 nm magnification and using the image J software program, the FE-SEM image (Fig. 3) shows that the particle size is between 30 nm and 50 nm. This image shows the morphology of the thin film of the Au NPs deposited on the silicon substrate. It is worth noting that the spherical arrays of the metallic nanoparticles can exhibit extremely narrow extinction rod-shaping excitations called surface lattice resonances (SLRs), which are a result of the coupling between LSPRs, coming from metallic nano-rods in the sample associated with individual nanoparticles and diffractive orders (DOs) present in periodic structures [30-33].

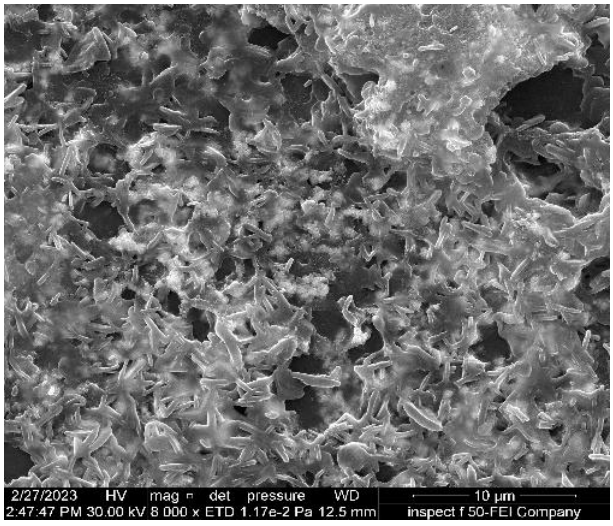

Figure 2: FE-SEM image of Au NPs (10 μm magnification).

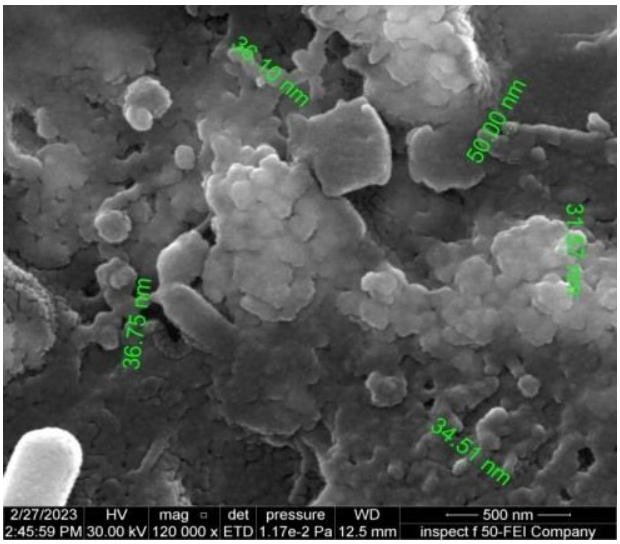

Figure 3: FE-SEM image of Au NPs (500 nm magnification).

The size of the AuNPs, shown in Table 2, was measured from the UV-visible spectrum using the Haiss equation [34]:

$$D = \frac{\ln \frac{\lambda_{SPR-\lambda_0}}{L1}}{L2} \quad (1)$$

where: λ_{spr} is the wavelength at maximum absorption, λ_o is the wavelength at minimum absorption occurring at the beginning of SPR and L1 and L2 are values taken from the data fit of the UV-visible spectrum. The size of the AuNPs was, on average, equal to 30 nm, and this result matches the FE-SEM image.

Table 2: Particle size of Au NPs measuring form UV-visible spectra

Seed (ml)	Particle size (nm)
10	30
12	29
15	30
18	31

Fig. 4 shows the UV-visible spectra of the AuNPs synthesized by the seed and growth method, in which the absorption appears at 532 nm. It is clear that the absorption increased with increasing seed size because the gold particle size increased. The seed-growth method indicated that by adding more seeds, the nanoparticles increased [35-41].

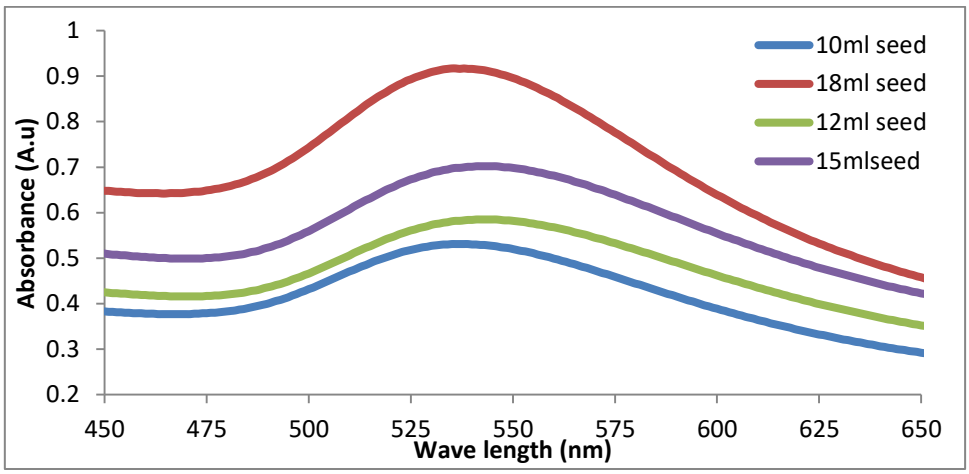

Figure 4: UV-Visible spectra of AuNPs.

Figs. 5-7 show the fluorescence spectra of the RhB dye-AuNPs mixture in different ratios. The fluorescence intensity of the mixture increased compared to that of the dye alone, and that of the 12 ml seed fell because of quenching. This quenching has occurred because of the reabsorption in this concentration of the 12 ml seed and the clear shifting of the fluorescence peak compared to that without AuNPs. This shifting happened toward shorter wavelengths (blue shift) because the nanoparticles increased the distance between the molecules, so the non-radiative process decreased, and the energy states of AuNPs and RhB overlapped, which was not easy to effect on the distance between the energy levels of Au NPs and RhB. The FHWM decreased compared to that without AuNPs because the stability of the dye molecules has increased due to the decrease in the molecule-molecule interaction. Because the energy

levels of the AuNPs and RhB overlapped, the concentration of 15 ml and 18 ml seeds had a lot of fluorescence. Also, the gap between energy levels S1 and S0 was bigger than it was for 10 ml and 12 ml seeds. The results of mixing nanoparticles with laser dye are consistent with the studies of Mutlak et al. [42-50].

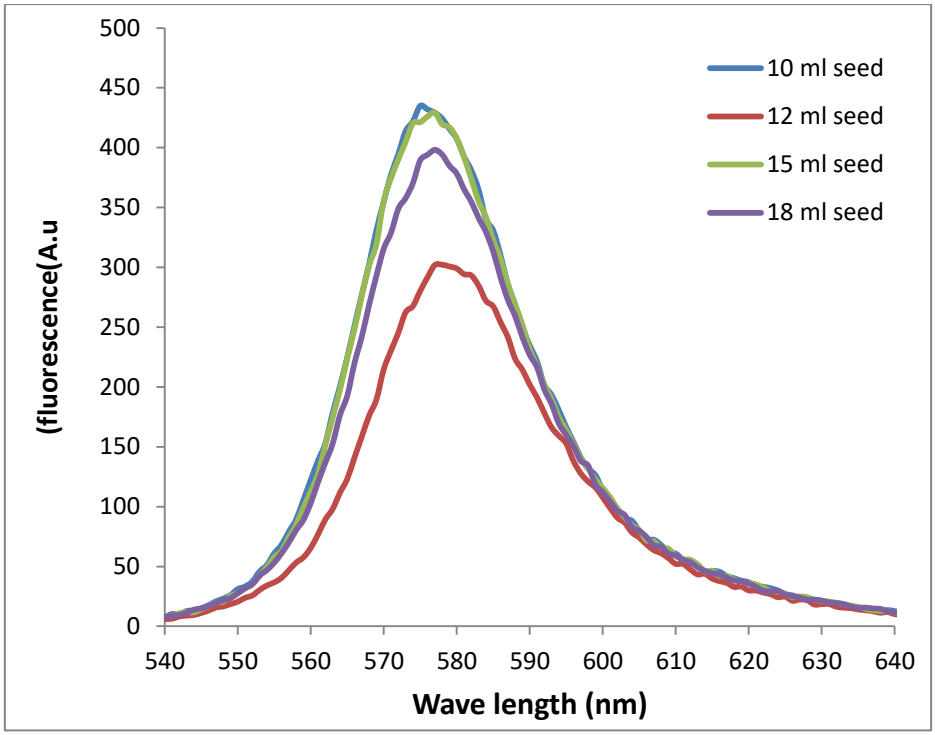

Figure 5: Fluorescence spectra of the RhB dye-AuNPs mixture of (1:1) mixing ratio.

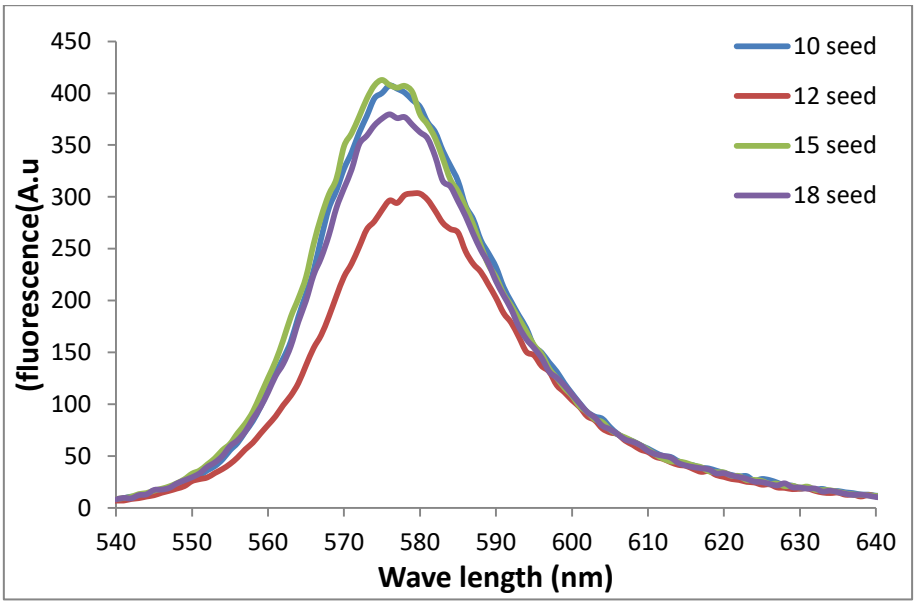

Figure 6: Fluorescence spectra of the RhB dye-AuNPs mixture of (1:2) mixing ratio.

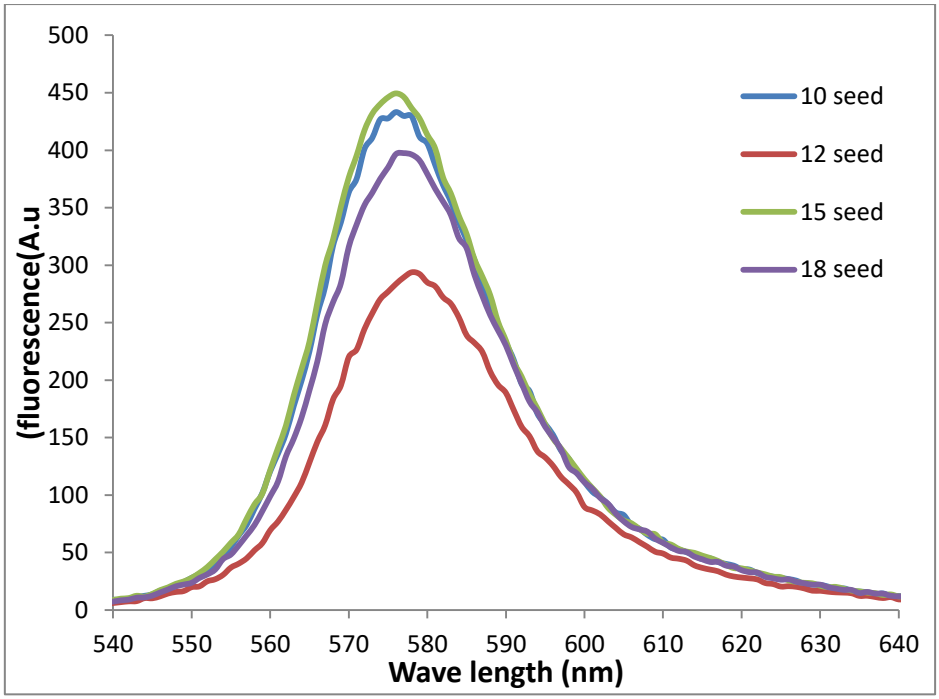

Figure 7: Fluorescence spectra of the RhB dye-AuNPs mixture of (1:3) mixing ratio.

4. Conclusions

The plasmonic phenomenon was evident in the emission spectra of the RhB dye-AuNPs mixture, indicating that the highest intensity was reached. However, the quenching process was evident for the 12 seed, in which the highest intensity showed that the increase in the concentration of AuNPs led to an increase in the plasmonic intensity and hence the localized surface plasmon phenomenon. In this study, XRD, FE-SEM, UV-Vis, and fluorescence measurements were used to analyze the gold nanoparticles produced by chemical reduction. It was established that AuNPs emerge as nano-stars with particles between 30 and 50 nm in size. RhB was added to the AuNPs to boost the intensity. This outcome has the potential to both enhance active media and create random gain media.

Acknowledgments

The authors would like to thank the department of physics, college of science, University of Baghdad, and Dr. Mohammed Abdullah Hameed and Dr. Sarmed M. Salah.

Conflict of interest

The authors declare that they have no conflict of interest.

References

1. G. Liu, D.-Q. Feng, Y. Qian, W. Wang, and J.-J. Zhu, Talanta **201**, 90 (2019).
2. M.-Z. Wei, T.-S. Deng, Q. Zhang, Z. Cheng, and S. Li, ACS omega **6**, 9188 (2021).
3. A. Kristensen, J. K. Yang, S. I. Bozhevolnyi, S. Link, P. Nordlander, N. J. Halas, and N. A. Mortensen, Natu. Rev. Mat. **2**, 1 (2016).
4. K. A. Willets and R. P. Van Duyne, Annu. Rev. Phys. Chem. **58**, 267 (2007).
5. K. Cai, W. Zhang, J. Zhang, H. Li, H. Han, and T. Zhai, ACS Appl. Mat. Inter. **10**, 36703 (2018).

6. A. Roy, C. Pandit, A. Gacem, M. S. Alqahtani, M. Bilal, S. Islam, M. J. Hossain, and M. Jameel, Bioinor. Chem. Appl. **2022**, 8184217 (2022).
7. S. Haddawi, H. R. Humud, and S. Hamidi, Optik **207**, 164482 (2020).
8. C. Yao and J. Zhu, J. Brazil. Chem. Soci. **31**, 589 (2020).
9. A. Prakash, J. C. Janardhanan, A. Padmakumar, V. K. Praveen, P. Radhakrishnan, and A. Mujeeb, J. Photochem. Photobio. A: Chem. **431**, 113997 (2022).
10. Z. Sadeq, A. Ali, and S. Al-Awadi, Int. J. Curr. Eng. Tech. **5**, 3170 (2015).
11. N. Hanžić, T. Jurkin, A. Maksimović, and M. Gotić, Rad. Phys. Chem. **106**, 77 (2015).
12. A. Sunatkari, S. Talwatkar, Y. Tamgadge, and G. Muley, Nanosci. Nanotech. **5**, 30 (2015).
13. F. A. Mutlak, M. Jaber, and H. Emad, Iraqi J. Sci. **58**, 2364 (2017).
14. W. Leng, P. Pati, and P. J. Vikesland, Envir. Sci.: Nano **2**, 440 (2015).
15. P. Prajapati, Y. Shah, and D. Sen, J. Chem. Pharm. Res. **2**, 30 (2010).
16. B. K. Nasser and M. A. Hameed, Nonlin. Opt., Quan. Opt.: Concep. Mod. Opt. **53**, 99 (2021).
17. M. A. Hameed, Iraqi J. Appl. Phys. **17**, 15 (2021).
18. M. A. Hameed and S. A. Akif, Iraqi J. Appl. Phys. **12**, 3 (2016).
19. A. A. Mohammed and M. A. Hameed, Iraqi J. Appl. Phys. **18**, 3 (2022).
20. M. R. Hashem and M. A. Hameed, Optik **260**, 169058 (2022).
21. E. C. Dreaden, L. A. Austin, M. A. Mackey, and M. A. El-Sayed, Therap. Deliv. **3**, 457 (2012).
22. S. J. Amina and B. Guo, Int. J. Nanomed. **15**, 9823 (2020).
23. C. Stanglmair, S. P. Scheeler, and C. Pacholski, Eur. J. Inorgan. Chem. **2014**, 3633 (2014).
24. X.-F. Hoo, K. A. Razak, N. S. Ridhuan, N. M. Nor, and N. D. Zakaria, in AIP Conference Proceedings, AIP Publishing, 2017, p. 030001.
25. A. Wang, H. P. Ng, Y. Xu, Y. Li, Y. Zheng, J. Yu, F. Han, F. Peng, and L. Fu, J. Nanomat. **2014**, 3 (2014).
26. W. Leng, P. Pati, and P. Vikesland, Envir. Sci.: Nano **2**, 440 (2015).
27. Y. Zhuang, L. Liu, X. Wu, Y. Tian, X. Zhou, S. Xu, Z. Xie, and Y. Ma, Partic. Sys. Charac. **36**, 1800077 (2019).
28. G. A. Vinnacombe-Willson, N. Chiang, P. S. Weiss, S. H. Tolbert, and L. Scarabelli, J. Chem. Edu. **98**, 546 (2020).
29. A. F. Ahmed, M. R. Abdulameer, M. M. Kadhim, and F. a.-H. Mutlak, Optik **249**, 168260 (2022).
30. E. M. Sulaiman, U. M. Nayef, and F. A. Mutlak, J. Opt., 1 (2022).
31. A. S. Alber and F. A. Mutlak, J. Opt., 1 (2022).
32. K. N. Patel, P. G. Trivedi, M. S. Thakar, K. V. Prajapati, D. K. Prajapati, and G. M. Sindhav, J. Gen. Eng. Biotech. **21**, 71 (2023).
33. A. A. Ashkarran, Plas. Sci. Tech. **15**, 376 (2013).
34. W. Haiss, N. T. Thanh, J. Aveyard, and D. G. Fernig, Anal. Chem. **79**, 4215 (2007).
35. Y. Raziani, P. Shakib, M. Rashidipour, K. Cheraghipour, J. Ghasemian Yadegari, and H. Mahmoudvand, Trop. Med. Infec. Dis. **8**, 313 (2023).
36. J. N. Chen, MSc. Thesis, Kent State University, (2012).
37. A. Khan, R. Rashid, G. Murtaza, and A. Zahra, Trop. J. Pharmaceut. Res. **13**, 1169 (2014).
38. M. A. Abed, F. A. Mutlak, A. F. Ahmed, U. M. Nayef, S. K. Abdulridha, and M. S. Jabir, in Journal of Physics: Conference Series, IOP Publishing, 2021, p. 012013.
39. A. W. Wahab, A. Karim, and I. W. Sutapa, Orien. J. Chem. **34**, 401 (2018).

40. P. Dobrowolska, A. Krajewska, M. Gajda-Rączka, B. Bartosewicz, P. Nyga, and B. J. Jankiewicz, Materials **8**, 2849 (2015).
41. D. Wu, J. Peng, Z. Cai, J. Weng, Z. Luo, N. Chen, and H. Xu, Opt. Expres. **23**, 24071 (2015).
42. M. R. Hashem and M. A. Hameed, Iraqi J. Appl. Phys. **18**, 35 (2022).
43. B. T. Chiad, M. A. Hameed, F. J. Kadhim, and K. H. Latif, Natu. Sci. **4**, 402 (2012).
44. M. Ahmad, W. Rehman, M. M. Khan, M. T. Qureshi, A. Gul, S. Haq, R. Ullah, A. Rab, and F. Menaa, J. Envir. Chem. Eng. **9**, 104725 (2021).
45. N. Guo, H. Liu, Y. Fu, and J. Hu, Optik **201**, 163537 (2020).
46. A. T. Dhiwahar, S. Maruthamuthu, R. Marnadu, M. Sundararajan, M. A. Manthrammel, M. Shkir, P. Sakthivel, and V. R. M. Reddy, Sol. Stat. Sci. **113**, 106542 (2021).
47. S. Kumar, S. Sharma, R. Kaushik, and L. Purohit, Mat. Today Chem. **20**, 100464 (2021).
48. L. A. Al-Bassam, Ph.D Thesis, University of Babylon, (2021).
49. A. A. Ali, MSc Thesis, Unvierstiy of Baghdad, (2022).
50. W. M. Alamier, M. Dy Oteef, A. M. Bakry, N. Hasan, K. S. Ismail, and F. S. J. a. O. Awad, ACS Omega **8**, 18901 (2023).

تحضير جسيمات الذهب النانوية واضافتها الى صبغه الرودامين الليزرية لتحسين الخصاص الطيفية للصبغة

ابو الحسن حاتم علي[1] و فلاح عبدالحسن مطلك[1]
[1]قسم الفيزياء، كلية العلوم، جامعة بغداد، بغداد، العراق

الخلاصة

في هذه الدراسة، تم تحضير عينات جزيئات النانو الذهبية بطريقة الاختزال الكيميائي (نمو البذور) مع 4 نسب (10، 12، 15 و 18) مل من البذور والنمو ثابت 40 مل. حيث تم دراسة الخصائص البصرية والتركيبية لهذه العينات. أظهرت عينة بذرة 18 مل أعلى امتصاص، وتم أخذ XRD لهذه العينات وظهرت ذروة واضحة عند (38.25^o, 44.5^o, 64.4^o, and 77.95^o) درجة. أظهرت الأشعة فوق البنفسجية المرئية أن امتصاص جميع العينات كان في نفس نطاق معيار Au NPs. أظهر FE-SEM شكل Au NPs كقضبان نانوية وحجم الجسيمات بين 30-50 نانومتر. ثم تم تحضير رودامين ب بتركيزM 10^{-5} ودُرست القياسات البصرية وتم اختيار أفضل طيف في التألق. ثم تم خلط Au NPs و RhB بنسب (1:1, 1:2, 1:3) وتم إجراء قياسات التألق. تم تغيير FHWM وشدة RhB بعد الخلط، وهذه النتيجة جيدة جدًا للعديد من التطبيقات. في هذه الدراسة، يمكن استخدام هذا الخلط بعد تعاطي المنشطات بالبوليمر كوسيط كسب عشوائي أو ممتص تشبع لتوليد الليزر النبضي.

الكلمات المفتاحية: الصبغات الليزرية، جسيمات الذهب النانوية، صبغة الرودامين ب، التحضير الكيميائي، الفلورة.